An annihilator-based strategy for the automatic detection of exponential polynomial spaces in subdivision

DOI:10.1016/j.cagd.2021.101976

An Annihilator-based Strategy for the Automatic Detection of Exponential Polynomial Spaces in Subdivision

Sergio López-Ureña[a,*], Alberto Viscardi[b,*]

[a] *Dep. de Matemàtiques, Universitat de València, Doctor Moliner Street 50, 46100 Burjassot, Valencia, Spain*
[b] *Dip. di Matematica, Alma Mater Studiorum Università di Bologna,Piazza P. S. Donato 5, 40126 Bologna, Italy*

Abstract

Exponential polynomials are essential in subdivision for the reconstruction of specific families of curves and surfaces, such as conic sections and quadric surfaces. It is well known that if a linear subdivision scheme is able to reproduce a certain space of exponential polynomials, then it must be level-dependent, with rules depending on the frequencies (and eventual multiplicities) defining the considered space. This work discusses a general strategy that exploits annihilating operators to locally detect those frequencies directly from the given data and therefore to choose the correct subdivision rule to be applied. This is intended as a first step towards the construction of self-adapting subdivision schemes able to locally reproduce exponential polynomials belonging to different spaces. An application of the proposed strategy is shown explicitly on an example involving the classical butterfly interpolatory scheme. This particular example is the generalization of what has been done for the univariate case in Donat and López-Ureña (2019), which inspired this work.

Keywords: annihilating operators, exponential polynomials, level-dependent subdivision

1. Introduction

This paper is concerned with the reproduction of *exponential polynomials* in a bivariate framework using recursive *subdivision schemes*. The reproduction of exponential polynomials is very important not only in connection with geometric modelling (to model shapes like conics or quadrics, see Beccari et al. (2007), Beccari et al. (2009), Lee and Yoon (2010) and Novara and Romani (2015)), but also in connection with applications like biomedical imaging (where sphere-like geometries naturally arise, see Uhlmann et al. (2014), Conti et al. (2015), Badoual et al. (2017a) and Badoual et al. (2017b)) or nuclear magnetic resonance spectroscopy data analysis (where multi-exponential decays frequently appear, see Li et al. (2015) and Campagna et al. (2020)). To reproduce shapes like conics or quadrics, subdivision schemes use two different strategies. The first consists in the construction of non-linear, geometrically-driven subdivision rules that are able to generate limit curves/surfaces sensitive to the geometry of the initial points (Sabin and Dodgson, 2005; Chalmovianský and Jüttler, 2007; Deng and Wang, 2010; Romani, 2010; Albrecht and Romani, 2012; Michálková and Bastl, 2015). The second relies on the definition of linear subdivision rules with the capability of reproducing exponential polynomials (Beccari et al., 2010; Conti and Romani, 2010; Conti et al., 2011, 2016a; Romani et al., 2016). Here, we follow the strategy in this second group of papers.

We remark that, even if the study of reproduction capabilities of subdivision schemes and their analysis are well developed in both the stationary and non stationary settings (see Charina et al. (2005), Conti et al. (2018) and Conti et al. (2019)), all available analysis tools require the preliminary knowledge of the space the scheme is capable to reproduce. Such a capability is also known to be connected to the approximation order of the scheme (see Levin (2005), Charina and Conti (2013), Jeong et al. (2013), Conti et al. (2016b), Novara et al. (2016) and references therein).

*Corresponding author
Email addresses: sergio.lopez-urena@uv.es (Sergio López-Ureña), alberto.viscardi@unibo.it (Alberto Viscardi)

In dimension $d \in \mathbb{N}$, a space of exponential polynomials is specified by a matrix of frequencies $\Gamma := [\boldsymbol{\gamma}_h]_{h=1}^{\nu} \in \mathbb{C}^{d\times\nu}$ with an associated matrix of corresponding multiplicities $M := [\mathbf{m}_h]_{h=1}^{\nu} \in \mathbb{N}^{d\times\nu}$, $\nu \in \mathbb{N}$ and it is defined as

$$W_{\Gamma,M} := \text{span}\left\{ \mathbf{x}^{\boldsymbol{\alpha}_h}\, e^{\boldsymbol{\gamma}_h^T\mathbf{x}} \,:\, \boldsymbol{\alpha}_h \text{ multi-index with } 0 \le \boldsymbol{\alpha}_h \le \mathbf{m}_h - 1 \right\}_{h=1}^{\nu}. \tag{1}$$

Up to now, in all subdivision schemes reproducing the space $W_{\Gamma,M}$, the level-dependent refinement rules involve explicitly the frequencies Γ and the corresponding multiplicities M. This is a major drawback since, usually, there is no a priori knowledge of the initial data, i.e., if they are samples of a function F in $W_{\Gamma,M}$, which prevents the choice of the right subdivision rules for the reconstruction of F. This problem is amplified considering shapes composed of different functions belonging to several exponential polynomial spaces. Indeed, in the latter situation, local values of the frequencies have to be detected from the initial data, since different subdivision rules have to be chosen locally for the exact reproduction of the different sections.

In Donat and López-Ureña (2019) this problem is addressed, in the univariate setting only, for a specific family of exponential polynomial spaces. In particular the authors constructed and analysed an interpolatory level-independent non-linear subdivision scheme reproducing the space

$$W_\gamma = \text{span}\{ 1,\, e^{\gamma x},\, e^{-\gamma x} \}, \qquad x \in \mathbb{R}, \tag{2}$$

for every $\gamma \in \mathbb{R}_{\ge 0} \cup i(0,\pi)$, where $i(0,\pi)$ denotes the open interval $\{it : t \in (0,\pi)\}$ on the imaginary axis. Their strategy exploits the orthogonal rules that annihilate the space (2). Orthogonal rules are one possible way to derive non-stationary subdivision schemes capable of reproducing spaces of exponential polynomials (see e.g. Dyn et al. (2003)). Indeed, in Donat and López-Ureña (2019), it is shown that from the orthogonal rules it is possible to derive the frequency γ as a function of the data attached to a stencil of the scheme.

The aim of this work is to illustrate a strategy for the automatic detection of frequencies (and eventual multiplicities) of exponential polynomial spaces in a very general *multidimensional* context. The presented approach is based on the so called annihilating operators, or annihilators, which generalize the concept of orthogonal rules (see the recent paper Conti et al. (2020)) to the multivariate setting.

To keep the exposition clear and to show the strength of this strategy in applications, a recurring example is considered in all sections. This pivotal example deals with exponential polynomial spaces of the form

$$W_{\boldsymbol{\gamma}} := \text{span}\{ 1,\, e^{\boldsymbol{\gamma}^T\mathbf{x}},\, e^{-\boldsymbol{\gamma}^T\mathbf{x}},\, e^{\widetilde{\boldsymbol{\gamma}}^T\mathbf{x}},\, e^{-\widetilde{\boldsymbol{\gamma}}^T\mathbf{x}} \}, \qquad \boldsymbol{\gamma} = \begin{bmatrix}\gamma_1\\ \gamma_2\end{bmatrix} \in \Omega^2, \qquad \widetilde{\boldsymbol{\gamma}} = \begin{bmatrix}\gamma_1\\ -\gamma_2\end{bmatrix}, \tag{3}$$

where

$$\Omega := \mathbb{R}_{\ge 0} \cup i(0,\pi), \tag{4}$$

in which spheres, cylinders, hyperboloids and other shapes can be described. We first provide linear level-dependent subdivision rules for the reconstruction of functions in $W_{\boldsymbol{\gamma}}$, starting from their samples on $\mathbb{Z}^2$. These rules depend on the frequency $\boldsymbol{\gamma}$. Then we construct a family of local annihilators that allow us to detect $\boldsymbol{\gamma}$ in a non-linear way from the data related to a single stencil of the scheme. The stencils here considered are the ones from the classical 8-point interpolatory subdivision scheme called *butterfly scheme* (Dyn et al., 1990). This is the natural extension to the bivariate case of what has been done in Donat and López-Ureña (2019).

The paper is organized as follows. In Section 2 we recall basic notions on subdivision schemes in a very general setting, introducing new notations when needed. The concept of step-wise reproduction is recalled in Section 3, where we also obtain the linear level-dependent rules needed to reproduce one $W_{\boldsymbol{\gamma}}$ in (3). Then, in Section 4 we provide a useful local family of annihilators for $\{W_{\boldsymbol{\gamma}}\}_{\boldsymbol{\gamma}\in\Omega^2}$ over $\mathbb{Z}^2$ and we use them to detect the frequency $\boldsymbol{\gamma}$ from the initial data attached to a single stencil of the butterfly scheme. We then summarize the tools needed in order to reproduce the used strategy for a general family of exponential polynomials (1). Finally, in Section 5, we show how the detection procedure in Section 4 can be further improved in order to detect the type of stencil associated to a finite ordered set of samples of an exponential polynomial.

2. Subdivision Preliminaries

Before recalling some standard facts about subdivision, the authors would like to inform the reader that, in order to make the proposed strategy as general as possible and to make the manuscript as consistent as possible, some non-standard notation is introduced. In particular, to deal with the general space of exponential polynomials (1), it is crucial to consider complex-valued sequences instead of real-valued ones.

Let $d \in \mathbb{N}$ and consider a sequence of discrete sets of distinct vertices $\{\Xi^{(k)} \subset \mathbb{R}^d\}_{k\in\mathbb{N}_0}$ ($\mathbb{N}_0 := \mathbb{N} \cup \{0\}$) so that there exists $\overline{\lim_{k\to\infty} \Xi^{(k)}} \;=\; D$ which is either $\mathbb{R}^d$ or a compact connected subset of it. In a very general setting, a *d-variate scalar subdivision scheme* $\mathcal{S} \;:=\; \{S^{(k)}\}_{k\in\mathbb{N}_0}$ is a sequence of *subdivision operators*, where, at each *subdivision level* k, $S^{(k)}$ refines sequences of data attached to $\Xi^{(k)}$ thus yielding sequences of data attached to $\Xi^{(k+1)}$, i.e.,

$$S^{(k)} \;:\; \ell(\Xi^{(k)},\mathbb{C}) \;\longrightarrow\; \ell(\Xi^{(k+1)},\mathbb{C}),$$

where $\ell(\Xi,\mathbb{C})$ denotes the set of sequences $\mathbf{f} = [f_\mathbf{j} \in \mathbb{C}]_{\mathbf{j}\in\Xi}$. We say that $\mathcal{S}$ is *convergent* if, for every set of initial data $\mathbf{f}^{(0)} \in \ell(\Xi^{(0)},\mathbb{C})$, the sequence of refined data $\{\mathbf{f}^{(k+1)} = S^{(k)}\,\mathbf{f}^{(k)}\}_{k\in\mathbb{N}_0}$, attached to the vertices $\Xi^{(k+1)}$, converges to the graph of a continuous function denoted as $S^\infty \mathbf{f}^{(0)}$.

A standard assumption in applications is that every subdivision operator acts locally, i.e. for every $\mathbf{j} \in \Xi^{(k+1)}$, there exists a finite ordered set $\mathcal{B}_\mathbf{j}^{(k)} \;\subset\; \Xi^{(k)}$, called *stencil*, and a function

$$\Psi_\mathbf{j}^{(k)} \;:\; \mathbb{C}^{n_\mathbf{j}^{(k)}} \;\longrightarrow\; \mathbb{C}, \qquad n_\mathbf{j}^{(k)} \;:=\; \#\mathcal{B}_\mathbf{j}^{(k)},$$

called *subdivision rule*, so that

$$f_\mathbf{j}^{(k+1)} \;=\; \Psi_\mathbf{j}^{(k)}\left(\mathbf{f}^{(k)}|_{\mathcal{B}_\mathbf{j}^{(k)}}\right), \qquad \forall \mathbf{j} \in \Xi^{(k+1)}. \tag{5}$$

Here, the restriction operator $\bullet|_{\mathcal{B}_\mathbf{j}^{(k)}} : \ell(\Xi^{(k)},\mathbb{C}) \to \mathbb{C}^{n_\mathbf{j}^{(k)}}$ is well defined because of the stencil $\mathcal{B}_\mathbf{j}^{(k)}$ being ordered.

Example 2.1. The classical butterfly scheme for the tri-directional grid can be described in this setting as follows:

(a) $d = 2$ and $D = \mathbb{R}^2$;

(b) for every $k \in \mathbb{N}_0$, $\Xi^{(k)} \;=\; 2^{-k}\mathbb{Z}^2$;

(c) for every $k \in \mathbb{N}_0$ and $\mathbf{j} \in \Xi^{(k+1)}$,

$$\mathcal{B}_\mathbf{j}^{(k)} \;=\; \begin{cases} \mathbf{j}, & \text{if } \mathbf{j} \in \Xi^{(k)}, \\ \mathbf{j} \,+\, 2^{-k-1}\left\{ \begin{bmatrix}-1\\0\end{bmatrix}, \begin{bmatrix}1\\0\end{bmatrix}, \begin{bmatrix}-1\\-2\end{bmatrix}, \begin{bmatrix}1\\2\end{bmatrix}, \begin{bmatrix}3\\2\end{bmatrix}, \begin{bmatrix}-1\\2\end{bmatrix}, \begin{bmatrix}-3\\-2\end{bmatrix}, \begin{bmatrix}1\\-2\end{bmatrix} \right\}, & \text{if } \mathbf{j} \in \frac{2\mathbb{Z}+1}{2^{k+1}} \times \frac{\mathbb{Z}}{2^k} \text{ (horizontal stencil)}, \\ \mathbf{j} \,+\, 2^{-k-1}\left\{ \begin{bmatrix}0\\-1\end{bmatrix}, \begin{bmatrix}0\\1\end{bmatrix}, \begin{bmatrix}-2\\-1\end{bmatrix}, \begin{bmatrix}2\\1\end{bmatrix}, \begin{bmatrix}2\\3\end{bmatrix}, \begin{bmatrix}2\\-1\end{bmatrix}, \begin{bmatrix}-2\\-3\end{bmatrix}, \begin{bmatrix}-2\\1\end{bmatrix} \right\}, & \text{if } \mathbf{j} \in \frac{\mathbb{Z}}{2^k} \times \frac{2\mathbb{Z}+1}{2^{k+1}} \text{ (vertical stencil)}, \\ \mathbf{j} \,+\, 2^{-k-1}\left\{ \begin{bmatrix}-1\\-1\end{bmatrix}, \begin{bmatrix}1\\1\end{bmatrix}, \begin{bmatrix}-1\\1\end{bmatrix}, \begin{bmatrix}1\\-1\end{bmatrix}, \begin{bmatrix}3\\1\end{bmatrix}, \begin{bmatrix}-1\\-3\end{bmatrix}, \begin{bmatrix}-3\\-1\end{bmatrix}, \begin{bmatrix}1\\3\end{bmatrix} \right\}, & \text{if } \mathbf{j} \in \frac{2\mathbb{Z}+1}{2^{k+1}} \times \frac{2\mathbb{Z}+1}{2^{k+1}} \text{ (diagonal stencil)}; \end{cases} \tag{6}$$

(d) for every $k \in \mathbb{N}_0$, if $\mathbf{j} \in \Xi^{(k+1)}$,

$$\begin{aligned} \Psi_\mathbf{j}^{(k)} \;:\; \mathbb{C} \;&\longrightarrow\; \mathbb{C} \\ z \;&\longmapsto\; z, \end{aligned}$$

otherwise,

$$\begin{aligned} \Psi_\mathbf{j}^{(k)} \;:\; \mathbb{C}^8 \;&\longrightarrow\; \mathbb{C} \\ \mathbf{z} \;=\; [z_h]_{h=1,\ldots,8} \;&\longmapsto\; \textstyle\sum_{h=1}^{8} a_h\, z_h \;=\; \mathbf{z}^T \mathbf{a}, \end{aligned}$$

with
$$\mathbf{a} \;=\; [a_h]_{h=1}^{8} \;=\; \left[\, \tfrac{1}{2},\quad \tfrac{1}{2},\quad \tfrac{1}{8},\quad \tfrac{1}{8},\quad -\tfrac{1}{16},\quad -\tfrac{1}{16},\quad -\tfrac{1}{16},\quad -\tfrac{1}{16} \right]^T. \tag{7}$$

The configurations of (c) and (d) for the horizontal, vertical and diagonal case are shown in Figure 1.

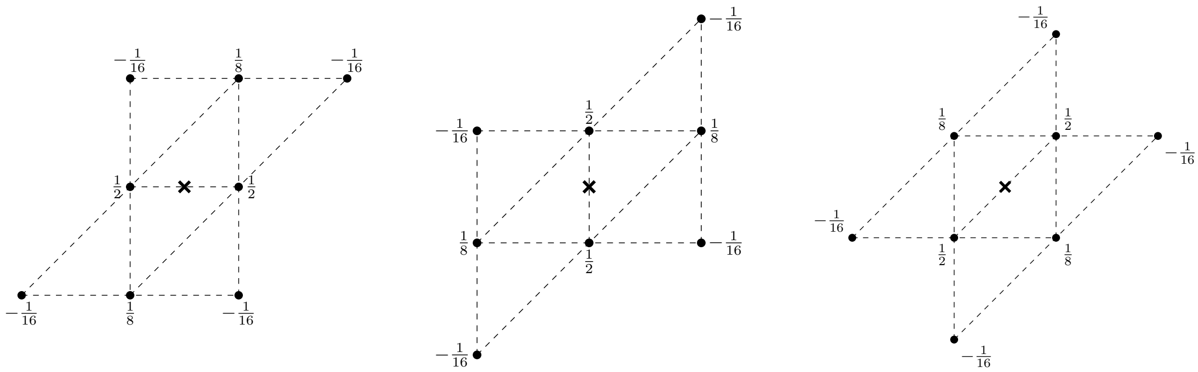

Figure 1: From left to right: the configuration of set $\mathcal{B}_{\mathbf{j}}^{(k)}$ related to the horizontal, vertical and diagonal case in (6), respectively. The cross indicates position $\mathbf{j}$, while the bullets illustrate the elements of $\mathcal{B}_{\mathbf{j}}^{(k)}$. The adjacent numbers are the corresponding elements of the mask (7).

The subdivision rules described in (d) do not depend on the subdivision level k (*level-independence*) nor on the vertex $\mathbf{j}$ (*shift-invariance*): there are essentially two different subdivision rules used at all subdivision levels, one for vertices already existing in the previous level (also known as *replacement rule*) and one for newly added vertices (also known as *insertion rule*). Moreover, these rules are linear operators. When this is the case, the vector $\mathbf{a}$ is called *mask* and the subdivision scheme is said to be *linear*.

Definition 2.1. We say that a subdivision scheme *reproduces* a set of functions $W \subset \{F : \mathbb{R}^d \longrightarrow \mathbb{C}\}$ on D if and only if, for every $F \in W$,

$$\mathbf{f}^{(0)} \;=\; F(\Xi^{(0)}) \;=\; [\, F(\mathbf{j}) \,]_{\mathbf{j}\in\Xi^{(0)}} \qquad \Longrightarrow \qquad S^{\infty}\,\mathbf{f}^{(0)} \;=\; F|_D. \tag{8}$$

For instance, the butterfly scheme described in Example 2.1 is able to reproduce polynomials with total degree up to 3 (see, e.g., Charina and Conti (2013)).

While some useful functions, like polynomials, can be reproduced using linear level-independent subdivision rules, to reproduce other interesting types of function, such as exponential polynomials, it is necessary to consider level-dependent subdivision rules.

3. Linear Level-dependent Rules for Exponential Polynomial Reproduction

Let $n \in \mathbb{N}$ and consider an n-dimensional space of functions W with basis $\{b_h : X \longrightarrow \mathbb{C}\}_{h=1,\ldots,n}$, i.e.

$$W \quad = \quad \mathrm{span}\{\, b_h \;:\; h = 1, \ldots, n \,\} \;=\; \{\, \textstyle\sum_{h=1}^{n} \, c_h\, b_h \;:\; c_h \in \mathbb{C} \,\},$$

where $X \subseteq \mathbb{R}^d$ is an open domain such that $\Xi^{(k)} \subset X$ for every $k \in \mathbb{N}_0$ (in particular $D \subseteq X$). If one wants to reproduce W on D with a subdivision scheme, a natural strategy is to ask a slightly stronger property than (8), namely:

Definition 3.1. We say that a subdivision scheme *stepwise reproduces* W if and only if, for every $F \in W$, $k \in \mathbb{N}_0$,

$$\mathbf{f}^{(k)} \;=\; F(\Xi^{(k)}) \qquad \Longrightarrow \qquad \mathbf{f}^{(k+1)} \;=\; F(\Xi^{(k+1)}). \tag{9}$$

In particular, if we seek linear subdivision rules, we have the following result.

Proposition 3.1. *Given* $\{\Xi^{(k)}\}_{k\in\mathbb{N}_0}$ *and* $\{\mathcal{B}_{\mathbf{j}}^{(k)}\}_{k\in\mathbb{N}_0,\mathbf{j}\in\Xi^{(k)}}$*, there exists a linear subdivision scheme stepwise reproducing the space* W*, with subdivision rules*

$$\Psi_{\mathbf{j}}^{(k)}(\mathbf{z}) \;=\; \sum_{h=1}^{n_{\mathbf{j}}^{(k)}} a_{\mathbf{j},h}^{(k)}\, z_h \;=\; \mathbf{z}^T\, \mathbf{a}_{\mathbf{j}}^{(k)}, \qquad k\in\mathbb{N}_0,\ \mathbf{j}\in\Xi^{(k+1)}, \tag{10}$$

for some $\mathbf{a}_{\mathbf{j}}^{(k)}\in\mathbb{C}^{n_{\mathbf{j}}^{(k)}}$ *if and only if, for every* $k\in\mathbb{N}_0$ *and* $\mathbf{j}\in\Xi^{(k+1)}$, $\mathbf{a}_{\mathbf{j}}^{(k)}$ *is a solution of*

$$\mathbf{V}_{\mathbf{j}}^{(k)}\, \mathbf{a}_{\mathbf{j}}^{(k)} \;=\; \mathbf{b}_{\mathbf{j}}, \tag{11}$$

where

$$\mathbf{b}_{\mathbf{j}} \;:=\; \big[b_h(\mathbf{j})\big]_{h=1}^{n} \;\in\; \mathbb{C}^n, \qquad \mathbf{V}_{\mathbf{j}}^{(k)} \;:=\; \big[\mathbf{b}_{\boldsymbol{\ell}}\big]_{\boldsymbol{\ell}\in\mathcal{B}_{\mathbf{j}}^{(k)}} \;\in\; \mathbb{C}^{n\times n_{\mathbf{j}}^{(k)}}.$$

Proof. The result follows from the fact that $\mathbf{V}_{\mathbf{j}}^{(k)}$ in (11) is an alternant matrix. Indeed, if

$$F(\mathbf{x}) \;=\; \sum_{h=1}^{n} c_h\, b_h(\mathbf{x}) \;\in\; W,$$

from (5) and (9) it follows that, for every $k\in\mathbb{N}_0$ and every $\mathbf{j}\in\Xi^{(k+1)}$,

$$F(\mathbf{j}) \;=\; f_{\mathbf{j}}^{(k+1)} \;=\; \Psi_{\mathbf{j}}^{(k)}\left(\mathbf{f}^{(k)}|_{\mathcal{B}_{\mathbf{j}}^{(k)}}\right) \;=\; \Psi_{\mathbf{j}}^{(k)}\left(\, F\left(\mathcal{B}_{\mathbf{j}}^{(k)}\right)\right).$$

This, due to (10), becomes

$$F(\mathbf{j}) \;=\; \big[F\left(\boldsymbol{\ell}\right)\big]_{\boldsymbol{\ell}\in\mathcal{B}_{\mathbf{j}}^{(k)}}^T\; \mathbf{a}_{\mathbf{j}}^{(k)}.$$

With $\mathbf{c}=[c_h]_{h=1}^n\in\mathbb{C}^n$, we can write $F(\mathbf{j}) \;=\; \mathbf{c}^T\,\mathbf{b}_{\mathbf{j}}$, for every $\mathbf{j}\in\Xi^{(k)}$, $k\in\mathbb{N}_0$. Thus, for every $\mathbf{c}\in\mathbb{C}^n$,

$$\mathbf{c}^T\,\mathbf{b}_{\mathbf{j}} \;=\; \mathbf{c}^T\,\mathbf{V}_{\mathbf{j}}^{(k)}\,\mathbf{a}_{\mathbf{j}}^{(k)},$$

which implies (11). The other implication is straightforward. □

Example 3.1. Let us construct a linear subdivision scheme with (a), (b) and (c) given as in the butterfly scheme in Section 2, that is able to reproduce on $\mathbb{R}^2$ the space $W_{\boldsymbol{\gamma}}$ in (3). To do so, we must study (11) for each of the four possible configurations of $\mathcal{B}_{\mathbf{j}}^{(k)}$ in (6). The case $\mathbf{j}\in\Xi^{(k)}$ is trivial, since it implies $\mathcal{B}_{\mathbf{j}}^{(k)}=\{\mathbf{j}\}$. Thus (11) becomes

$$\mathbf{b}_{\mathbf{j}}\,\mathbf{a}_{\mathbf{j}}^{(k)} \;=\; \mathbf{b}_{\mathbf{j}} \qquad\Longrightarrow\qquad \mathbf{a}_{\mathbf{j}}^{(k)} \;=\; 1 \qquad\Longrightarrow\qquad \Psi_{\mathbf{j}}^{(k)}(z) \;=\; z.$$

Let us now consider the horizontal case. The resulting system (11) is underdetermined since $\mathbf{V}_{\mathbf{j}}^{(k)}\in\mathbb{C}^{5\times 8}$ and it is possible to show that, asking for the same symmetries as (7), there exists a unique solution $\mathbf{a}_{\mathbf{j}}^{(k)} \;=\; [a_{\mathbf{j},h}^{(k)}]_{h=1}^8$ with

$$\begin{cases} a_{\mathbf{j},1}^{(k)} \;=\; a_{\mathbf{j},2}^{(k)} \;=\; \frac{1}{2\phi_1^{(k)}}, \\[2ex] a_{\mathbf{j},3}^{(k)} \;=\; a_{\mathbf{j},4}^{(k)} \;=\; \frac{2(\phi_1^{(k)})^2-1}{4\phi_1^{(k)}\left(\phi_1^{(k)}+1\right)}, \\[2ex] a_{\mathbf{j},5}^{(k)} \;=\; a_{\mathbf{j},6}^{(k)} \;=\; a_{\mathbf{j},7}^{(k)} \;=\; a_{\mathbf{j},8}^{(k)} \;=\; -\frac{1}{8\phi_1^{(k)}\left(\phi_1^{(k)}+1\right)}, \end{cases} \tag{12}$$

where $\phi_1^{(k)} := \cosh\left(2^{-k-1}\gamma_1\right)$. The vertical case can be obtained from the horizontal one by exchanging the role of γ_1 and γ_2, thus replacing $\phi_1^{(k)}$ in (12) with $\phi_2^{(k)} := \cosh\left(2^{-k-1}\gamma_2\right)$. The setting for the diagonal case is the same, an underdetermined system with 5 equations and 8 unknowns that, under symmetry requirements, admits the unique solution $\mathbf{a}_{\mathbf{j}}^{(k)} = [a_{\mathbf{j},h}^{(k)}]_{h=1}^{8}$ with

$$\begin{cases} a_{\mathbf{j},1}^{(k)} = a_{\mathbf{j},2}^{(k)} = \frac{2\phi_1^{(k)}\phi_2^{(k)}\left((\phi_1^{(k)})^2+(\phi_2^{(k)})^2-1\right)-(\phi_1^{(k)})^2-(\phi_2^{(k)})^2}{4\phi_1^{(k)}\phi_2^{(k)}\left((\phi_1^{(k)})^2+(\phi_2^{(k)})^2-2\right)}, \\ a_{\mathbf{j},3}^{(k)} = a_{\mathbf{j},4}^{(k)} = \frac{(\phi_1^{(k)})^2+(\phi_2^{(k)})^2-\phi_1^{(k)}\phi_2^{(k)}-1}{4\phi_1^{(k)}\phi_2^{(k)}\left((\phi_1^{(k)})^2+(\phi_2^{(k)})^2-2\right)}, \\ a_{\mathbf{j},5}^{(k)} = a_{\mathbf{j},6}^{(k)} = a_{\mathbf{j},7}^{(k)} = a_{\mathbf{j},8}^{(k)} = \frac{1-\phi_1^{(k)}\phi_2^{(k)}}{8\phi_1^{(k)}\phi_2^{(k)}\left((\phi_1^{(k)})^2+(\phi_2^{(k)})^2-2\right)}. \end{cases} \tag{13}$$

Remark 3.1. For the practical implementation of rules (12) and (13), one has to carefully deal with the cases where the rules are not well defined, i.e. when, for $k \in \mathbb{N}_0$, one of the following holds

$$\Phi_1^{(k)},\ \Phi_2^{(k)} \in \{\,0,\ -1\,\} \qquad \text{or} \qquad \left(\Phi_1^{(k)}\right)^2 + \left(\Phi_2^{(k)}\right)^2 - 2 = 0.$$

This however overtakes the aim of this work which, referring to this specific example, is to detect $\boldsymbol{\gamma}$ from the samples $\mathbf{f}^{(0)} = F(\Xi^{(0)})$ of a function $F \in W_{\boldsymbol{\gamma}}$, for some $\boldsymbol{\gamma} \in \Omega^2$.

As expected, since the basis of $W_{\boldsymbol{\gamma}}$ depends on the frequency $\boldsymbol{\gamma}$, the resulting subdivision rules given by (12) and (13) also depend on it, in the form of $\phi_1^{(k)}$ and $\phi_2^{(k)}$, which also depend on the subdivision level k (but not on $\mathbf{j}$). On the other hand, in order to use such subdivision rules, one has only to compute $\phi_1^{(0)}$ and $\phi_2^{(0)}$, since

$$\phi_h^{(k)} = \cosh\left(\frac{\gamma_h}{2^{k+1}}\right) = \sqrt{\frac{\cosh\left(\frac{\gamma_h}{2^k}\right)+1}{2}} = \sqrt{\frac{\phi_h^{(k-1)}+1}{2}}, \qquad k \in \mathbb{N},\ h = 1, 2. \tag{14}$$

The fact that we were able to obtain (12) and (13) depending only on $\phi_1^{(k)}$ and $\phi_2^{(k)}$ is heavily related to the structure of $\{\Xi^{(k)}\}_{k\in\mathbb{N}_0}$, $\{\mathcal{B}_{\mathbf{j}}^{(k)}\}_{k\in\mathbb{N}_0,\mathbf{j}\in\Xi^{(k+1)}}$ and $W_{\boldsymbol{\gamma}}$. For general sets of vertices, stencils and spaces of exponential polynomials $W_{\Gamma,M}$ as in (1), if there exists $\mathbf{a}_{\mathbf{j}}^{(k)}$, for every $k \in \mathbb{N}_0$ and $\mathbf{j} \in \Xi^{(k+1)}$, solving (11), it will have a much more complicated expression in terms of the elements of Γ and M.

4. Annihilating Operators and Parameters Detection

In contrast to Section 2 and 3, in which a general setting was first built and then specialized in Example 2.1 and 3.1, respectively, here we follow a different approach. To get the reader acquainted to the proposed strategy, we present first how the detection of the frequency $\boldsymbol{\gamma}$ for the family of spaces $\{W_{\boldsymbol{\gamma}}\}_{\boldsymbol{\gamma}\in\Omega^2}$ in (3) can be done for the specific setting in Example 2.1 and 3.1. Then a description of the procedure in the general setting is given. This should allow the reader to get an intuition about the tools and the properties needed for the general case.

Example 4.1. Consider the setting described by Example 2.1 and 3.1. As proven in Conti et al. (2020), for every $\boldsymbol{\gamma} \in \Omega^2$, $\mathbf{v}_0, \mathbf{v}_1, \mathbf{v}_2, \mathbf{v}_3, \mathbf{v}_4 \in \mathbb{R}^2$,

$$\Delta_{\mathbf{v}_0}^{0}\, \Delta_{\mathbf{v}_1}^{\boldsymbol{\gamma}}\, \Delta_{\mathbf{v}_2}^{-\boldsymbol{\gamma}}\, \Delta_{\mathbf{v}_3}^{\widetilde{\boldsymbol{\gamma}}}\, \Delta_{\mathbf{v}_4}^{-\widetilde{\boldsymbol{\gamma}}}\, F(\mathbf{x}) = 0, \qquad \forall F \in W_{\boldsymbol{\gamma}},\ \mathbf{x} \in \mathbb{R}^2, \tag{15}$$

where

$$\Delta_{\mathbf{v}}^{\boldsymbol{\gamma}}\, F(\mathbf{x}) := F(\mathbf{x}+\mathbf{v}) - e^{\boldsymbol{\gamma}^T\mathbf{v}}\, F(\mathbf{x}). \tag{16}$$

Because of the structure of (16), the left-hand-side of (15) involves the samples of F at the points

$$\{\,\mathbf{x}\,+\,\epsilon_0\mathbf{v}_0\,+\,\epsilon_1\mathbf{v}_1\,+\,\epsilon_2\mathbf{v}_2\,+\,\epsilon_3\mathbf{v}_3\,+\,\epsilon_4\mathbf{v}_4\;:\;\epsilon_h\in\{0,1\},\;h\in\{0,\ldots,4\}\,\}\,.$$

We consider now the discrete analogue of (15), keeping the same notation when possible to underline the analogy with the continuous case. Since $\Xi^{(0)}=\mathbb{Z}^2$, for every $\mathbf{x},\mathbf{v}_0,\mathbf{v}_1,\mathbf{v}_2,\mathbf{v}_3,\mathbf{v}_4\in\mathbb{Z}^2$, the operator

$$\begin{array}{rcccl}\mathcal{N}_{\mathbf{x},\mathbf{v}_0,\mathbf{v}_1,\mathbf{v}_2,\mathbf{v}_3,\mathbf{v}_4} & : & \Omega^2\times\ell(\Xi^{(0)},\mathbb{C}) & \longrightarrow & \mathbb{C}\\ & & (\boldsymbol{\gamma},\mathbf{f}) & \longmapsto & \Delta^{0}_{\mathbf{v}_0}\,\Delta^{\boldsymbol{\gamma}}_{\mathbf{v}_1}\,\Delta^{-\boldsymbol{\gamma}}_{\mathbf{v}_2}\,\Delta^{\widetilde{\boldsymbol{\gamma}}}_{\mathbf{v}_3}\,\Delta^{-\widetilde{\boldsymbol{\gamma}}}_{\mathbf{v}_4}\,\mathbf{f}\,\big|_{\mathbf{x}}\,,\end{array}\tag{17}$$

where

$$\begin{array}{rcccl}\Delta^{\boldsymbol{\gamma}}_{\mathbf{v}} & : & \ell(\Xi^{(0)},\mathbb{C}) & \longrightarrow & \ell(\Xi^{(0)},\mathbb{C})\\ & & \mathbf{f} & \longmapsto & \tau_{\mathbf{v}}\mathbf{f}\,-\,e^{\boldsymbol{\gamma}^T\mathbf{v}}\,\mathbf{f},\end{array}\qquad\begin{array}{rcccl}\tau_{\mathbf{v}} & : & \ell(\Xi^{(0)},\mathbb{C}) & \longrightarrow & \ell(\Xi^{(0)},\mathbb{C})\\ & & \mathbf{f}=[f_{\mathbf{j}}]_{\mathbf{j}\in\Xi^{(0)}} & \longmapsto & \mathbf{g}=[g_{\mathbf{j}}=f_{\mathbf{j}+\mathbf{v}}]_{\mathbf{j}\in\Xi^{(0)}}\,,\end{array}$$

is called an *annihilator for* $\{W_{\boldsymbol{\gamma}}\}_{\boldsymbol{\gamma}\in\Omega^2}$ *on* $\Xi^{(0)}$, since, for every $F\in W_{\boldsymbol{\gamma}}$, $\boldsymbol{\gamma}\in\Omega^2$, it satisfies

$$\mathcal{N}_{\mathbf{x},\mathbf{v}_0,\mathbf{v}_1,\mathbf{v}_2,\mathbf{v}_3,\mathbf{v}_4}\Big(\boldsymbol{\gamma},F(\Xi^{(0)})\Big)=0.$$

Remark 4.1. With an abuse of notation but without ambiguity, the restriction operator $|$ is used at the end of (17) without parenthesis, even if it is applied as the last operator in the chain, after the operators of the form $\Delta^{\boldsymbol{\gamma}}_{\mathbf{v}}$. In what follows, this convention is maintained in similar situations to make the notation less cumbersome.

Each annihilator of the form (17) is identified by an element of $\mathbb{Z}^{12}$, since $\mathbf{x},\mathbf{v}_0,\mathbf{v}_1,\mathbf{v}_2,\mathbf{v}_3$ and $\mathbf{v}_4$ can be chosen as arbitrary vectors in $\mathbb{Z}^2$. To proceed with the computations, we restrict ourselves to a very special subfamily of (17) that is enough to detect the frequency $\boldsymbol{\gamma}$ and is noteworthy for other properties. Let us define, for $\mathbf{x},\mathbf{v},\mathbf{e}\in\Xi^{(0)}$, the operator

$$\begin{array}{rcccl}\mathcal{N}_{\mathbf{x},\mathbf{v},\mathbf{e}} & : & \Omega^2\times\ell(\Xi^{(0)},\mathbb{C}) & \longrightarrow & \mathbb{C}\\ & & (\boldsymbol{\gamma},\mathbf{f}) & \longmapsto & \Delta^{0}_{\mathbf{v}}\,\Delta^{\boldsymbol{\gamma}}_{\mathbf{e}}\,\Delta^{-\boldsymbol{\gamma}}_{\mathbf{e}}\,\mathbf{f}\,|_{\mathbf{x}}.\end{array}\tag{18}$$

Now, for

$$\mathbf{e}_1\;:=\;\begin{bmatrix}1\\0\end{bmatrix}\qquad\text{and}\qquad\mathbf{e}_2\;:=\;\begin{bmatrix}0\\1\end{bmatrix},$$

one can observe that

$$\Delta^{\boldsymbol{\gamma}}_{\mathbf{e}_1}\;=\;\Delta^{\widetilde{\boldsymbol{\gamma}}}_{\mathbf{e}_1},\qquad\Delta^{\boldsymbol{\gamma}}_{\mathbf{e}_2}\;=\;\Delta^{-\widetilde{\boldsymbol{\gamma}}}_{\mathbf{e}_2},\qquad\Delta^{-\boldsymbol{\gamma}}_{\mathbf{e}_1}\;=\;\Delta^{-\widetilde{\boldsymbol{\gamma}}}_{\mathbf{e}_1}\quad\text{and}\quad\Delta^{-\boldsymbol{\gamma}}_{\mathbf{e}_2}\;=\;\Delta^{\widetilde{\boldsymbol{\gamma}}}_{\mathbf{e}_2}.\tag{19}$$

According to (19), it can be proved that also the operators $\mathcal{N}_{\mathbf{x},\mathbf{v},\mathbf{e}_1}$ and $\mathcal{N}_{\mathbf{x},\mathbf{v},\mathbf{e}_2}$ annihilate $\{W_{\boldsymbol{\gamma}}\}_{\boldsymbol{\gamma}\in\Omega^2}$ on $\Xi^{(0)}$ for every $\mathbf{x},\mathbf{v}\in\mathbb{Z}^2$ (see Conti et al. (2020) for details). Of particular interest are the annihilators of the form

$$\mathcal{N}_{\mathbf{x},\mathbf{e}_1+2\mathbf{e}_2,\mathbf{e}_1},\quad\mathcal{N}_{\mathbf{x},\mathbf{e}_1,\mathbf{e}_2},\quad\mathcal{N}_{\mathbf{x},\mathbf{e}_2,\mathbf{e}_1},\quad\mathcal{N}_{\mathbf{x},2\mathbf{e}_1+\mathbf{e}_2,\mathbf{e}_2},\quad\mathcal{N}_{\mathbf{x},\mathbf{e}_1+\mathbf{e}_2,\mathbf{e}_1}\quad\text{and}\quad\mathcal{N}_{\mathbf{x},\mathbf{e}_1+\mathbf{e}_2,\mathbf{e}_2},\tag{20}$$

because they are pairwise related to the horizontal (the first and the second operator), vertical (the third and the fourth operator) and diagonal stencils (the fifth and the last operator) in (6), respectively. This is a consequence of the following result.

Proposition 4.1. *For every* $\mathbf{x},\mathbf{v},\mathbf{e}\in\Xi^{(0)}$,

$$\begin{aligned}\mathcal{N}_{\mathbf{x},\mathbf{v},\mathbf{e}}(\boldsymbol{\gamma},\mathbf{f})\;&=\;-2\cosh(\boldsymbol{\gamma}^T\mathbf{e})\;\Delta^0_{\mathbf{v}}\mathbf{f}\,\big|_{\mathbf{x}+\mathbf{e}}\;+\;\Delta^0_{\mathbf{v}}\mathbf{f}\,\big|_{\mathbf{x}+2\mathbf{e}}\;+\;\Delta^0_{\mathbf{v}}\mathbf{f}\,\big|_{\mathbf{x}}\\&=\;\mathbf{c}^T\;\mathbf{f}|_{\mathcal{B}}\,,\end{aligned}\tag{21}$$

where

$$\mathbf{c} \;=\; \left[\, -2\cosh(\boldsymbol{\gamma}^T\mathbf{e}),\quad 2\cosh(\boldsymbol{\gamma}^T\mathbf{e}),\quad 1,\quad -1,\quad 1,\quad -1 \right]^T,$$
$$\mathcal{B} \;=\; \mathbf{x} + \{\, \mathbf{v}+\mathbf{e},\ \mathbf{e},\ \mathbf{v}+2\mathbf{e},\ 2\mathbf{e},\ \mathbf{v},\ \mathbf{0} \,\}\,.$$

In particular, for $\mathbf{f}^{(0)} = F(\Xi^{(0)})$*,* $F \in W_{\boldsymbol{\gamma}}$*,* $\boldsymbol{\gamma} \in \Omega^2$ *and* $\Delta^0_{\mathbf{v}}\mathbf{f}^{(0)}\,\big|_{\mathbf{x}+\mathbf{e}} \neq 0$*,*

$$\cosh(\boldsymbol{\gamma}^T\mathbf{e}) \;=\; \frac{\Delta^0_{\mathbf{v}}\mathbf{f}^{(0)}\,\big|_{\mathbf{x}+2\mathbf{e}} \;+\; \Delta^0_{\mathbf{v}}\mathbf{f}^{(0)}\,\big|_{\mathbf{x}}}{2\;\;\Delta^0_{\mathbf{v}}\mathbf{f}^{(0)}\,\big|_{\mathbf{x}+\mathbf{e}}}. \tag{22}$$

Proof. From definition (17) we get

$$\begin{aligned}
\mathcal{N}_{\mathbf{x},\mathbf{v},\mathbf{e}}(\boldsymbol{\gamma},\mathbf{f}) \;&=\; \Delta^0_{\mathbf{v}}\;\Delta^{\boldsymbol{\gamma}}_{\mathbf{e}}\;\Delta^{-\boldsymbol{\gamma}}_{\mathbf{e}}\;\mathbf{f}\,\big|_{\mathbf{x}}\\
&=\; \Delta^0_{\mathbf{v}}\;\Delta^{\boldsymbol{\gamma}}_{\mathbf{e}_1}\;(\tau_{\mathbf{e}}\mathbf{f} \;-\; e^{-\boldsymbol{\gamma}^T\mathbf{e}}\;\mathbf{f})\,\Big|_{\mathbf{x}}\\
&=\; \Delta^0_{\mathbf{v}}\;\Big(\,\tau_{\mathbf{e}}(\tau_{\mathbf{e}}\mathbf{f} \;-\; e^{-\boldsymbol{\gamma}^T\mathbf{e}}\;\mathbf{f}) - e^{\boldsymbol{\gamma}^T\mathbf{e}}(\tau_{\mathbf{e}}\mathbf{f} \;-\; e^{-\boldsymbol{\gamma}^T\mathbf{e}}\;\mathbf{f})\,\Big)\,\Big|_{\mathbf{x}}\\
&=\; \Delta^0_{\mathbf{v}}\;\big(\,\tau_{\mathbf{e}}\tau_{\mathbf{e}}\mathbf{f} \;-\; 2\cosh(\boldsymbol{\gamma}^T\mathbf{e})\tau_{\mathbf{e}}\mathbf{f} \;+\; \mathbf{f}\,\big)\,\big|_{\mathbf{x}}\\
&=\; -2\cosh(\boldsymbol{\gamma}^T\mathbf{e})\;\;\Delta^0_{\mathbf{v}}\mathbf{f}\,\big|_{\mathbf{x}+\mathbf{e}} \;+\; \Delta^0_{\mathbf{v}}\mathbf{f}\,\big|_{\mathbf{x}+2\mathbf{e}} \;+\; \Delta^0_{\mathbf{v}}\mathbf{f}\,\big|_{\mathbf{x}}\,,
\end{aligned}$$

where for the last equality we exploit the fact that $\Delta^0_{\mathbf{v}}\tau_{\mathbf{e}} = \tau_{\mathbf{e}}\Delta^0_{\mathbf{v}}$. Moreover, since $\mathcal{N}_{\mathbf{x},\mathbf{v},\mathbf{e}}$ is an annihilator for $\{W_{\boldsymbol{\gamma}}\}_{\boldsymbol{\gamma}\in\Omega^2}$ over $\Xi^{(0)}$, $\mathcal{N}_{\mathbf{x},\mathbf{v},\mathbf{e}}(\boldsymbol{\gamma},\mathbf{f}^{(0)}) = 0$. Thus, if $\Delta^0_{\mathbf{v}}\mathbf{f}\,\big|_{\mathbf{x}+\mathbf{v}} \neq 0$, (21) can be solved for $\cosh(\boldsymbol{\gamma}^T\mathbf{e})$ so obtaining (22). ☐

As a consequence of (21), we get the following expressions for the operators in (20):

$$\begin{aligned}
\mathcal{N}_{\mathbf{x},\mathbf{e}_1+2\mathbf{e}_2,\mathbf{e}_1}(\boldsymbol{\gamma},\mathbf{f}) \;&=\; 2\cosh(\gamma_1)\,(\,f_{\mathbf{x}+\mathbf{e}_1} \;-\; f_{\mathbf{x}+2\mathbf{e}_1+2\mathbf{e}_2}\,) \;+\; f_{\mathbf{x}+3\mathbf{e}_1+2\mathbf{e}_2} \;+\; f_{\mathbf{x}+\mathbf{e}_1+2\mathbf{e}_2} \;-\; f_{\mathbf{x}+2\mathbf{e}_1} \;-\; f_{\mathbf{x}},\\
\mathcal{N}_{\mathbf{x},\mathbf{e}_1,\mathbf{e}_2}(\boldsymbol{\gamma},\mathbf{f}) \;&=\; 2\cosh(\gamma_2)\,(\,f_{\mathbf{x}+\mathbf{e}_2} \;-\; f_{\mathbf{x}+\mathbf{e}_1+\mathbf{e}_2}\,) \;+\; f_{\mathbf{x}+\mathbf{e}_1\,+\,2\mathbf{e}_2} \;+\; f_{\mathbf{x}+\mathbf{e}_1} \;-\; f_{\mathbf{x}+2\mathbf{e}_2} \;-\; f_{\mathbf{x}},\\
\mathcal{N}_{\mathbf{x},\mathbf{e}_2,\mathbf{e}_1}(\boldsymbol{\gamma},\mathbf{f}) \;&=\; 2\cosh(\gamma_1)\,(\,f_{\mathbf{x}+\mathbf{e}_1} \;-\; f_{\mathbf{x}+\mathbf{e}_1+\mathbf{e}_2}\,) \;+\; f_{\mathbf{x}+2\mathbf{e}_1+\mathbf{e}_2} \;+\; f_{\mathbf{x}+\mathbf{e}_2} \;-\; f_{\mathbf{x}+2\mathbf{e}_1} \;-\; f_{\mathbf{x}},\\
\mathcal{N}_{\mathbf{x},2\mathbf{e}_1+\mathbf{e}_2,\mathbf{e}_2}(\boldsymbol{\gamma},\mathbf{f}) \;&=\; 2\cosh(\gamma_2)\,(\,f_{\mathbf{x}+\mathbf{e}_2} \;-\; f_{\mathbf{x}+2\mathbf{e}_1+2\mathbf{e}_2}\,) \;+\; f_{\mathbf{x}+2\mathbf{e}_1+3\mathbf{e}_2} \;+\; f_{\mathbf{x}+2\mathbf{e}_1+\mathbf{e}_2} \;-\; f_{\mathbf{x}+2\mathbf{e}_2} \;-\; f_{\mathbf{x}},\\
\mathcal{N}_{\mathbf{x},\mathbf{e}_1+\mathbf{e}_2,\mathbf{e}_1}(\boldsymbol{\gamma},\mathbf{f}) \;&=\; 2\cosh(\gamma_1)\,(\,f_{\mathbf{x}+\mathbf{e}_1} \;-\; f_{\mathbf{x}+2\mathbf{e}_1+\mathbf{e}_2}\,) \;+\; f_{\mathbf{x}+3\mathbf{e}_1+\mathbf{e}_2} \;+\; f_{\mathbf{x}+\mathbf{e}_1+\mathbf{e}_2} \;-\; f_{\mathbf{x}+2\mathbf{e}_1} \;-\; f_{\mathbf{x}},\\
\mathcal{N}_{\mathbf{x},\mathbf{e}_1+\mathbf{e}_2,\mathbf{e}_2}(\boldsymbol{\gamma},\mathbf{f}) \;&=\; 2\cosh(\gamma_2)\,(\,f_{\mathbf{x}+\mathbf{e}_2} \;-\; f_{\mathbf{x}+\mathbf{e}_1+2\mathbf{e}_2}\,) \;+\; f_{\mathbf{x}+\mathbf{e}_1+3\mathbf{e}_2} \;+\; f_{\mathbf{x}+\mathbf{e}_1+\mathbf{e}_2} \;-\; f_{\mathbf{x}+2\mathbf{e}_2} \;-\; f_{\mathbf{x}}.
\end{aligned}$$

In particular, for $\mathbf{j} \in (2\mathbb{Z}{+}1)/2{\times}\mathbb{Z}$ (horizontal stencil), we have that $\mathcal{N}_{\mathbf{j}-3\mathbf{e}_1/2-\mathbf{e}_2,\mathbf{e}_1+2\mathbf{e}_2,\mathbf{e}_1}$ and $\mathcal{N}_{\mathbf{j}-\mathbf{e}_1/2-\mathbf{e}_2,\mathbf{e}_1,\mathbf{e}_2}$ require only elements of $\mathbf{f}|_{\mathcal{B}^{(0)}_{\mathbf{j}}}$ to be computed. Moreover, when well defined, (22) gives us

$$\left\{\begin{aligned}
\cosh(\gamma_1) \;&=\; \frac{f^{(0)}_{\mathbf{j}+3\mathbf{e}_1/2+\mathbf{e}_2} + f^{(0)}_{\mathbf{j}-\mathbf{e}_1/2+\mathbf{e}_2} - f^{(0)}_{\mathbf{j}+\mathbf{e}_1/2-\mathbf{e}_2} - f^{(0)}_{\mathbf{j}-3\mathbf{e}_1/2-\mathbf{e}_2}}{2\Big(\,f^{(0)}_{\mathbf{j}-\mathbf{e}_1/2-\mathbf{e}_2} - f^{(0)}_{\mathbf{j}+\mathbf{e}_1/2+\mathbf{e}_2}\,\Big)},\\[2ex]
\cosh(\gamma_2) \;&=\; \frac{f^{(0)}_{\mathbf{j}+\mathbf{e}_1/2+\mathbf{e}_2} + f^{(0)}_{\mathbf{j}+\mathbf{e}_1/2-\mathbf{e}_2} - f^{(0)}_{\mathbf{j}-\mathbf{e}_1/2+\mathbf{e}_2} - f^{(0)}_{\mathbf{j}-\mathbf{e}_1/2-\mathbf{e}_2}}{2\Big(\,f^{(0)}_{\mathbf{j}-\mathbf{e}_1/2} - f^{(0)}_{\mathbf{j}+\mathbf{e}_1/2}\,\Big)}.
\end{aligned}\right. \tag{23}$$

The same can be done for $\mathbf{j} \in \mathbb{Z} \times (2\mathbb{Z}+1)/2$ (vertical stencil), $\mathcal{N}_{\mathbf{j}-\mathbf{e}_1-\mathbf{e}_2/2,\mathbf{e}_2,\mathbf{e}_1}$ and $\mathcal{N}_{\mathbf{j}-\mathbf{e}_1-3\mathbf{e}_2/2,2\mathbf{e}_1+\mathbf{e}_2,\mathbf{e}_2}$, obtaining

$$\left\{\begin{aligned}
\cosh(\gamma_1) \;&=\; \frac{f^{(0)}_{\mathbf{j}+\mathbf{e}_1+\mathbf{e}_2/2} + f^{(0)}_{\mathbf{j}-\mathbf{e}_1+\mathbf{e}_2/2} - f^{(0)}_{\mathbf{j}+\mathbf{e}_1-\mathbf{e}_2/2} - f^{(0)}_{\mathbf{j}-\mathbf{e}_1-\mathbf{e}_2/2}}{2\Big(\,f^{(0)}_{\mathbf{j}-\mathbf{e}_2/2} - f^{(0)}_{\mathbf{j}+\mathbf{e}_2/2}\,\Big)},\\[2ex]
\cosh(\gamma_2) \;&=\; \frac{f^{(0)}_{\mathbf{j}+\mathbf{e}_1+3\mathbf{e}_2/2} + f^{(0)}_{\mathbf{j}+\mathbf{e}_1-\mathbf{e}_2/2} - f^{(0)}_{\mathbf{j}-\mathbf{e}_1+\mathbf{e}_2/2} - f^{(0)}_{\mathbf{j}-\mathbf{e}_1-3\mathbf{e}_2/2}}{2\Big(\,f^{(0)}_{\mathbf{j}-\mathbf{e}_1-\mathbf{e}_2/2} - f^{(0)}_{\mathbf{j}+\mathbf{e}_1+\mathbf{e}_2/2}\,\Big)},
\end{aligned}\right. \tag{24}$$

and for $\mathbf{j} \in (2\mathbb{Z}+1)/2 \times (2\mathbb{Z}+1)/2$ (diagonal stencil), $\mathcal{N}_{\mathbf{j}-3\mathbf{e}_1/2-\mathbf{e}_2/2,\mathbf{e}_1+\mathbf{e}_2,\mathbf{e}_1}$ and $\mathcal{N}_{\mathbf{j}-\mathbf{e}_1/2-3\mathbf{e}_2/2,\mathbf{e}_1+\mathbf{e}_2,\mathbf{e}_2}$, obtaining

$$\begin{cases} \cosh(\gamma_1) &= \dfrac{f^{(0)}_{\mathbf{j}+3\mathbf{e}_1/2+\mathbf{e}_2/2} + f^{(0)}_{\mathbf{j}-\mathbf{e}_1/2+\mathbf{e}_2/2} - f^{(0)}_{\mathbf{j}+\mathbf{e}_1/2-\mathbf{e}_2/2} - f^{(0)}_{\mathbf{j}-3\mathbf{e}_1/2-\mathbf{e}_2/2}}{2\left(f^{(0)}_{\mathbf{j}-\mathbf{e}_1/2-\mathbf{e}_2/2} - f^{(0)}_{\mathbf{j}+\mathbf{e}_1/2+\mathbf{e}_2/2} \right)}, \\[2ex] \cosh(\gamma_2) &= \dfrac{f^{(0)}_{\mathbf{j}+\mathbf{e}_1/2+3\mathbf{e}_2/2} + f^{(0)}_{\mathbf{j}+\mathbf{e}_1/2-\mathbf{e}_2/2} - f^{(0)}_{\mathbf{j}-\mathbf{e}_1/2+\mathbf{e}_2/2} - f^{(0)}_{\mathbf{j}-\mathbf{e}_1/2-3\mathbf{e}_2/2}}{2\left(f^{(0)}_{\mathbf{j}-\mathbf{e}_1/2-\mathbf{e}_2/2} - f^{(0)}_{\mathbf{j}+\mathbf{e}_1/2+\mathbf{e}_2/2} \right)}. \end{cases} \tag{25}$$

The configurations of vertices involved in these equations are shown in Figure 2.

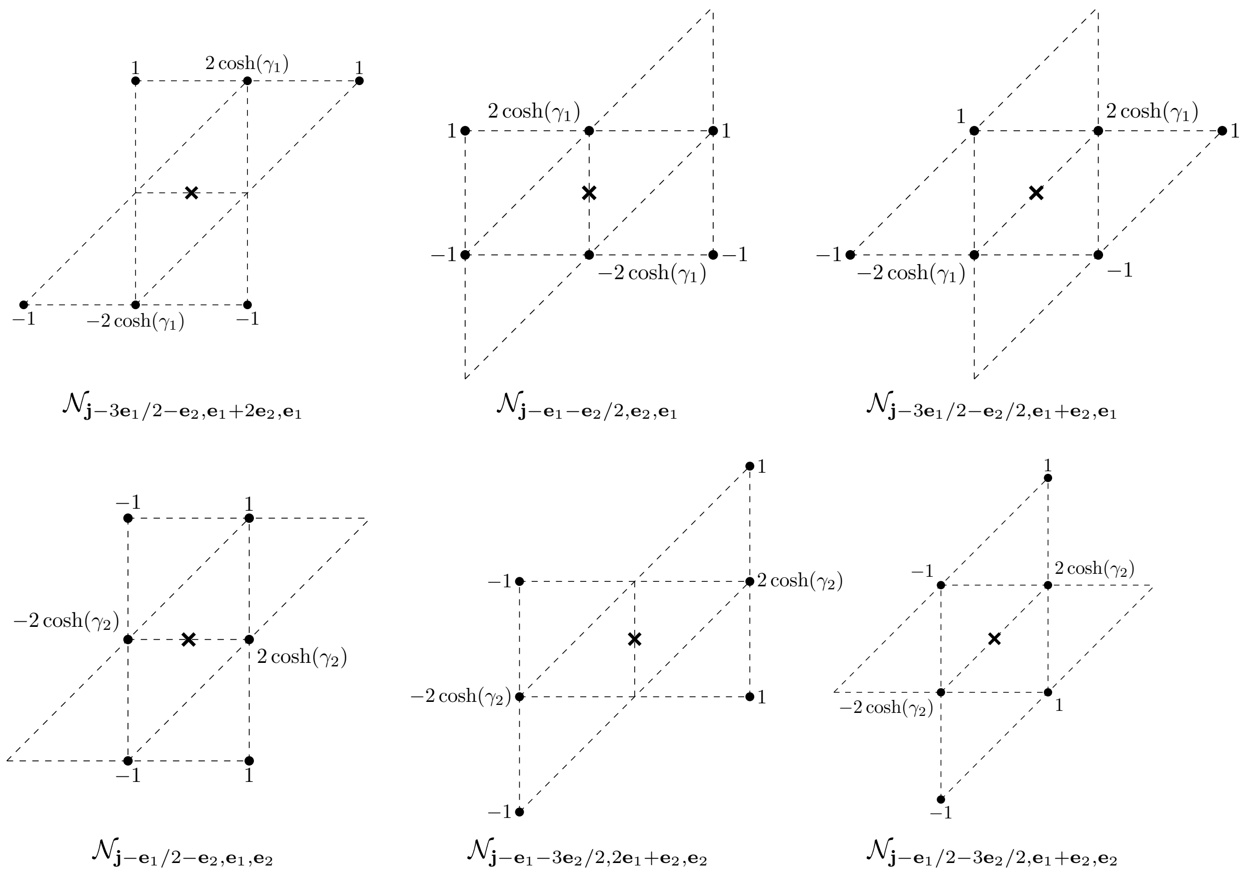

Figure 2: The configuration of the vertices involved in the local annihilators for the detection of $\cosh(\gamma_1)$ (on the top row) and $\cosh(\gamma_2)$ (on the bottom row), in the case of $\mathcal{B}^{(0)}_{\mathbf{j}}$, $\mathbf{j} \in \Xi^{(1)} \setminus \Xi^{(0)}$, being an horizontal stencil (first column, (23)), a vertical stencil (central column, (24)) or a diagonal stencil (third column, (25)), where the cross indicates the vertex $\mathbf{j}$.

Remark 4.2. One way to deal with the cases when (23), (24) or (25) are not well defined is to consider more local annihilators in order to get a one-to-one correspondence between a solution $(\boldsymbol{\gamma}, \mathbf{f})$ for the system given by all the annihilators and a function in $\{W_{\boldsymbol{\gamma}}\}_{\boldsymbol{\gamma}\in\Omega^2}$. This is also the strategy presented in Section 5 to solve another issue, and is presented there in more details (see Remark 5.1).

Remark 4.3. Since, $\Xi^{(k)} = 2^{-k}\Xi^{(0)}$ and $F \in W_{\boldsymbol{\gamma}} \Leftrightarrow F(2^{-k}\cdot) \in W_{2^{-k}\boldsymbol{\gamma}}$, for every $k \in \mathbb{N}$, equations (23), (24) and (25) can be recast for $\phi_1^{(k-1)} = \cosh(2^{-k}\gamma_1)$ and $\phi_2^{(k-1)} = \cosh(2^{-k}\gamma_2)$ simply substituting $\mathbf{f}^{(0)}$ with $\mathbf{f}^{(k)}$. The resulting subdivision rules obtained combining (12) and (13) with (23), (24) and (25) are then non-linear and level-independent.

Remark 4.4. The choice of Ω^2 in (4) as the set of frequencies is natural in the following sense. Since for applications we are interested in real-valued sequences $\mathbf{f}^{(0)}$, from (23), (24) and (25) follows that $\cosh(\gamma_h) \in$

$\mathbb{R}$, for $h = 1, 2$, and this is true if and only if $\gamma_h \in (\mathbb{R} + i\pi\mathbb{Z}) \cup i\mathbb{R}$. In order to get a one-to-one correspondence between $[\cosh(\gamma_1), \cosh(\gamma_2)]^T$ and the space $W_{\boldsymbol{\gamma}}$ in (3), considering the periodicity of the cosine function, the fact that $W_{\boldsymbol{\gamma}} = W_{-\boldsymbol{\gamma}} = W_{\widetilde{\boldsymbol{\gamma}}} = W_{-\widetilde{\boldsymbol{\gamma}}}$ and the recurrence relation (14), it is natural to consider $\gamma_h \in \mathbb{R}_{\geq 0} \cup i(0, \pi)$, $h = 1, 2$, for the detection procedure here described.

To summarize, starting from a class of annihilators for the samples of functions in $\{W_{\boldsymbol{\gamma}}\}_{\boldsymbol{\gamma} \in \Omega^2}$ over $\Xi^{(0)} = \mathbb{Z}^2$, we were able to find equations that can be used to detect the frequency $\boldsymbol{\gamma}$ directly from the initial data $\mathbf{f}^{(0)}$. These equations are also local, in the sense that they only involve vertices coming from a single stencil $\mathcal{B}_{\mathbf{j}}^{(0)}$, $\mathbf{j} \in \Xi^{(1)}$, thus they could be even used to detect different frequencies for samples of piecewise functions with pieces belonging to different function spaces $W_{\boldsymbol{\gamma}}$ (see, e.g., Figure 4).

In the general case, suppose to have a sequence of vertices $\{\Xi^{(k)}\}_{k \in \mathbb{N}_0}$, a set of stencils $\{\mathcal{B}_{\mathbf{j}}^{(k)}\}_{k \in \mathbb{N}_0, \mathbf{j} \in \Xi^{(k+1)}}$ and a set of frequencies and multiplicities $\widehat{\Omega} \subset \mathbb{C}^{d \times \nu} \times \mathbb{N}^{d \times \nu}$, and let $\{\mathbf{a}_{\mathbf{j}}^{(k)}\}_{k \in \mathbb{N}_0, \mathbf{j} \in \Xi^{(k+1)}}$, depending on Γ and M, be such that the associated linear subdivision scheme is able to stepwise reproduce the family of exponential polynomial spaces $\{W_{\Gamma,M}\}_{(\Gamma,M) \in \widehat{\Omega}}$ as in (1). Given $\mathbf{f}^{(0)} = F(\Xi^{(0)})$ for some $F \in W_{\Gamma,M}$ with $(\Gamma, M) \in \widehat{\Omega}$ unknown, in order to use the correct subdivision rules to reproduce F, our goal is to detect (Γ, M) directly from $\mathbf{f}^{(0)}$. To do so we define *annihilating operators*, as in Example 4.1.

Definition 4.1. Let $\mathcal{B}$ be a set of vertices. An operator $\mathcal{N} : \widehat{\Omega} \times \ell(\mathcal{B}, \mathbb{C}) \longrightarrow \mathbb{C}$ is said to be an *annihilator* for the family of spaces $\{W_{\Gamma,M}\}_{(\Gamma,M) \in \widehat{\Omega}}$ over $\mathcal{B}$ if and only if, for every $(\Gamma, M) \in \widehat{\Omega}$,

$$\mathcal{N}\left((\Gamma, M), F(\mathcal{B})\right) \;=\; 0, \qquad \forall F \in W_{\Gamma,M}.$$

Every annihilator $\mathcal{N}$ of $\{W_{\Gamma,M}\}_{(\Gamma,M) \in \widehat{\Omega}}$ over $\Xi^{(0)}$ then provides an equation of the form

$$0 \;=\; \mathcal{N}\left((\Gamma, M), F(\Xi^{(0)})\right) \;=\; \mathcal{N}((\Gamma, M), \mathbf{f}^{(0)}),$$

involving only the data $\mathbf{f}^{(0)}$ and the unknown frequencies and multiplicities (Γ, M). Thus, a family of annihilators $\{\mathcal{N}_h\}_{h \in \mathcal{I}}$, where $\mathcal{I}$ is a set of indices, yields a system of equations with the same unknowns. The equations involved are in general non-linear and the possibility to solve the system for Γ and M heavily depends on the structure of the annihilators. The construction of *good* annihilators has therefore a critical role and it has to be investigated case by case. To do so, exploiting the symmetries of the set of vertices, the stencils and the considered spaces can be crucial, as shown in Example 4.1, in order to obtain useful results for applications, such as local formulas for the detection of frequencies.

5. Stencil-type Detection

For the classical butterfly scheme in Example 2.1, the subdivision rules (d) distinguish only stencils that consist of a single vertex from stencils given by a set of 8 ordered vertices. In particular, there is a unique rule for all the 8-point stencil, namely horizontal, vertical and diagonal. Thus, for $k \in \mathbb{N}_0$, $\mathbf{f}^{(k)} \in \ell(\Xi^{(k)}, \mathbb{C})$, $\mathbf{j} \in \Xi^{(k+1)}$, given $\mathbf{p} = \mathbf{f}^{(k)}|_{\mathcal{B}_{\mathbf{j}}^{(k)}} \in \mathbb{C}^8$ there is no ambiguity in applying the subdivision rule (7), no matter the type of stencil $\mathcal{B}_{\mathbf{j}}^{(k)}$. Instead, as for Example 3.1, we have three different rules, defined in (12) and (13), that must be applied depending on $\mathcal{B}_{\mathbf{j}}^{(k)}$ being horizontal, vertical or diagonal, respectively. All these different types of stencils consist of 8 ordered points that have the same topological structure (Figure 3, plain bullets). Thus, if we are given only $\mathbf{p} \in \mathbb{C}^8$, without information about the type of stencil $\mathbf{p}$ is attached to, there is ambiguity with respect to the correct subdivision rule to be used on it. The same holds for Example 4.1, since there we obtained three different systems of equations, (23), (24) and (25), to detect $\boldsymbol{\gamma} \in \Omega^2$ using data attached to a horizontal, a vertical or a diagonal stencil, respectively, that can all be applied to a generic data vector $\mathbf{p} \in \mathbb{C}^8$.

In a general setting, suppose to have a set $\mathcal{T}$ of different types of stencils, all with cardinality $H \in \mathbb{N}$ and the same topological configuration. It is natural to ask the following question: is it possible, given only

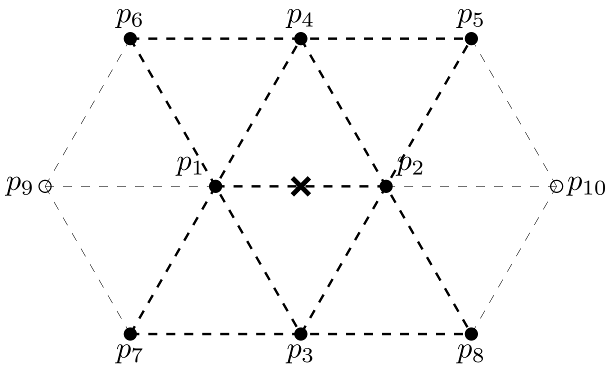

Figure 3: The generic topological configuration of the ordered data $\mathbf{p} = [p_h]_{h=1}^{10} \in \mathbb{C}^{10}$, with $\mathbf{p} = \mathbf{f}^{(k)}|_{\mathcal{B}_{\mathbf{j}}^{(k)}}$, attached to the stencil $\mathcal{B}_{\mathbf{j}}^{(k)}$, input for the extended insertion rule to compute the new vertex $\mathbf{j} \in \Xi^{(k+1)} \setminus \Xi^{(k)}$ (cross). The plain bullets denote the data for the stencils of the classical butterfly scheme (Example 2.1 (c)), while the empty bullets denote the two added points needed for stencil-type detection (Example 5.1 (c')).

$\mathbf{p} \in \mathbb{C}^H$, to determine the correct stencil-type $t \in \mathcal{T}$ in order to choose the right equations for the detection of the frequencies (and the eventual multiplicities) and the correct subdivision rule? Annihilators prove themselves useful again to answer this question. As for Section 4, we first show how this can be done for the setting introduced in Example 2.1, 3.1 and 4.1 and then we highlight the crucial points of this strategy to be used in the general setting.

Example 5.1. In order to achieve the desired result, for reasons that will be clear soon, we need to consider slightly bigger stencils than the ones defined in Example 2.1. In particular, we substitute (c) with

(c') for every $k \in \mathbb{N}_0$ and $\mathbf{j} \in \Xi^{(k+1)}$,

$$\mathcal{B}_{\mathbf{j}}^{(k)} = \begin{cases} \mathbf{j}, & \text{if } \mathbf{j} \in \Xi^{(k)}, \\ \mathbf{j} + 2^{-k-1}\left\{\begin{bmatrix}-1\\0\end{bmatrix}, \begin{bmatrix}1\\0\end{bmatrix}, \begin{bmatrix}-1\\-2\end{bmatrix}, \begin{bmatrix}1\\2\end{bmatrix}, \begin{bmatrix}3\\2\end{bmatrix}, \begin{bmatrix}-1\\2\end{bmatrix}, \begin{bmatrix}-3\\-2\end{bmatrix}, \begin{bmatrix}1\\-2\end{bmatrix}, \begin{bmatrix}-3\\0\end{bmatrix}, \begin{bmatrix}3\\0\end{bmatrix}\right\}, & \text{if } \mathbf{j} \in \frac{2\mathbb{Z}+1}{2^{k+1}} \times \frac{\mathbb{Z}}{2^k} \text{ (horizontal stencil)}, \\ \mathbf{j} + 2^{-k-1}\left\{\begin{bmatrix}0\\-1\end{bmatrix}, \begin{bmatrix}0\\1\end{bmatrix}, \begin{bmatrix}-2\\-1\end{bmatrix}, \begin{bmatrix}2\\1\end{bmatrix}, \begin{bmatrix}2\\3\end{bmatrix}, \begin{bmatrix}2\\-1\end{bmatrix}, \begin{bmatrix}-2\\-3\end{bmatrix}, \begin{bmatrix}-2\\1\end{bmatrix}, \begin{bmatrix}0\\-3\end{bmatrix}, \begin{bmatrix}0\\3\end{bmatrix}\right\}, & \text{if } \mathbf{j} \in \frac{\mathbb{Z}}{2^k} \times \frac{2\mathbb{Z}+1}{2^{k+1}} \text{ (vertical stencil)}, \\ \mathbf{j} + 2^{-k-1}\left\{\begin{bmatrix}-1\\-1\end{bmatrix}, \begin{bmatrix}1\\1\end{bmatrix}, \begin{bmatrix}-1\\1\end{bmatrix}, \begin{bmatrix}1\\-1\end{bmatrix}, \begin{bmatrix}3\\1\end{bmatrix}, \begin{bmatrix}-1\\-3\end{bmatrix}, \begin{bmatrix}-3\\-1\end{bmatrix}, \begin{bmatrix}1\\3\end{bmatrix}, \begin{bmatrix}-3\\-3\end{bmatrix}, \begin{bmatrix}3\\3\end{bmatrix}\right\}, & \text{if } \mathbf{j} \in \frac{2\mathbb{Z}+1}{2^{k+1}} \times \frac{2\mathbb{Z}+1}{2^{k+1}} \text{ (diagonal stencil)}. \end{cases} \tag{26}$$

Namely, the horizontal, vertical and diagonal stencils now have two additional points, which make them coincide with the stencils of the so called *extended butterfly scheme*. The shared topology of these three different types of stencils is shown in Figure 3. The linear rules (7), (12) and (13) can be extended accordingly simply setting to 0 the coefficients related to the two newly added points.

Without loss of generality, consider $k = 0$. For the local detection of $\boldsymbol{\gamma}$, in Example 4.1 we exploited the annihilators (20). These annihilators involve data from a single stencil of the classical butterfly scheme and we extracted all the information they could give us detecting $\boldsymbol{\gamma}$ in (23), (24) and (25). Given $\mathbf{p} \in \mathbb{C}^8$, we can apply all these equations, setting $\mathbf{f}^{(0)}|_{\mathcal{B}_{\mathbf{j}}^{(0)}} = \mathbf{p}$, and obtain three different values for $\boldsymbol{\gamma}$ in Ω^2 that we call $\boldsymbol{\gamma}_{hori}$, $\boldsymbol{\gamma}_{vert}$ and $\boldsymbol{\gamma}_{diag}$, respectively.

The idea now is to obtain, again via annihilators, further conditions to test which, between $\boldsymbol{\gamma}_{hori}$, $\boldsymbol{\gamma}_{vert}$ and $\boldsymbol{\gamma}_{diag}$, is the correct one to be chosen. To do so, we need more annihilators. Unfortunately, the ones in the family (18) are not enough. For instance, for the diagonal case, the annihilators used in (25) are the unique ones belonging to the family (18) that are supported in a single diagonal stencil of the classical butterfly scheme. Thus, in order to have more annihilators available, we are forced to introduce two additional points to each stencil associated with an insertion rule as described in (26). This way we can also consider operators of the following forms

$$\begin{array}{rcccl} \mathcal{N}^+_{\mathbf{x},\mathbf{v}_0,\mathbf{v}_1,\mathbf{v}_2,\mathbf{v}_3} & : & \Omega^2 \times \ell(\Xi^{(0)},\mathbb{C}) & \longrightarrow & \mathbb{C} \\ & & (\boldsymbol{\gamma},\mathbf{f}) & \longmapsto & \Delta^0_{\mathbf{v}_0}\, \Delta^{\gamma}_{\mathbf{v}_1}\, \Delta^{-\gamma}_{\mathbf{v}_2}\, \Delta^{\widetilde{\gamma}}_{\mathbf{v}_3}\, \mathbf{f}\,|_{\mathbf{x}}, \end{array} \tag{27}$$

and

$$\begin{array}{rcccl} \mathcal{N}^-_{\mathbf{x},\mathbf{v}_0,\mathbf{v}_1,\mathbf{v}_2,\mathbf{v}_3} & : & \Omega^2 \times \ell(\Xi^{(0)},\mathbb{C}) & \longrightarrow & \mathbb{C} \\ & & (\boldsymbol{\gamma},\mathbf{f}) & \longmapsto & \Delta^0_{\mathbf{v}_0}\, \Delta^{\gamma}_{\mathbf{v}_1}\, \Delta^{-\gamma}_{\mathbf{v}_2}\, \Delta^{-\widetilde{\gamma}}_{\mathbf{v}_3}\, \mathbf{f}\,|_{\mathbf{x}}, \end{array} \tag{28}$$

where $\mathbf{x}$, $\mathbf{v}_0$, $\mathbf{v}_1$, $\mathbf{v}_2$, $\mathbf{v}_3 \in \mathbb{Z}^2$. As for equation (21) in Proposition 4.1, one can prove that (27) and (28) act on $\mathbf{f}$ in a linear way. Moreover, suitable choices of $\mathbf{x}$, $\mathbf{v}_0$, $\mathbf{v}_1$, $\mathbf{v}_2$, $\mathbf{v}_3 \in \mathbb{Z}^2$ make them local annihilators of $W_{\boldsymbol{\gamma}}$ over $\Xi^{(0)}$ involving data in a single stencil $\mathcal{B}^{(0)}_{\mathbf{j}}$. In particular, for $\mathbf{j} \in \Xi^{(1)} \setminus \Xi^{(0)}$, we consider the following local annihilators: for the horizontal case,

$$\mathcal{N}_{\mathbf{j}-3\mathbf{e}_1/2,\mathbf{e}_1,\mathbf{e}_1}, \qquad \mathcal{N}^+_{\mathbf{j}-3\mathbf{e}_1/2-\mathbf{e}_2,\mathbf{e}_1,\mathbf{e}_2,\mathbf{e}_1,\mathbf{e}_1+\mathbf{e}_2}, \qquad \mathcal{N}^-_{\mathbf{j}-3\mathbf{e}_1/2-\mathbf{e}_2,\mathbf{e}_1,\mathbf{e}_1,\mathbf{e}_2,\mathbf{e}_1+\mathbf{e}_2}; \tag{29}$$

for the vertical case,

$$\mathcal{N}_{\mathbf{j}-3\mathbf{e}_2/2,\mathbf{e}_2,\mathbf{e}_2}, \qquad \mathcal{N}^+_{\mathbf{j}-\mathbf{e}_1-3\mathbf{e}_2/2,\mathbf{e}_2,\mathbf{e}_1,\mathbf{e}_2,\mathbf{e}_1+\mathbf{e}_2}, \qquad \mathcal{N}^-_{\mathbf{j}-\mathbf{e}_1-3\mathbf{e}_2/2,\mathbf{e}_2,\mathbf{e}_2,\mathbf{e}_1,\mathbf{e}_1+\mathbf{e}_2}; \tag{30}$$

for the diagonal case,

$$\mathcal{N}^+_{\mathbf{j}-3\mathbf{e}_1/2-3\mathbf{e}_2/2,\mathbf{e}_1+\mathbf{e}_2,\mathbf{e}_2,\mathbf{e}_1,\mathbf{e}_1+\mathbf{e}_2}, \quad \mathcal{N}^+_{\mathbf{j}-3\mathbf{e}_1/2-3\mathbf{e}_2/2,\mathbf{e}_1,\mathbf{e}_2,\mathbf{e}_1+\mathbf{e}_2,\mathbf{e}_1+\mathbf{e}_2}, \quad \mathcal{N}^-_{\mathbf{j}-3\mathbf{e}_1/2-3\mathbf{e}_2/2,\mathbf{e}_1,\mathbf{e}_1+\mathbf{e}_2,\mathbf{e}_2,\mathbf{e}_1+\mathbf{e}_2}. \tag{31}$$

Since all the stencils $\{\mathcal{B}^{(0)}_{\mathbf{j}}\}_{\mathbf{j}\in\Xi^{(1)}\setminus\Xi^{(0)}}$ have cardinality 10, annihilators in (29), (30) and (31) can be seen naturally as operators acting on $\Omega^2 \times \mathbb{C}^{10}$ instead of $\Omega^2 \times \ell(\Xi^{(0)},\mathbb{C})$.

The reason why we choose three additional annihilators for each case is the following. Without loss of generality, due to the shift-invariance of the space $W_{\boldsymbol{\gamma}}$, $\boldsymbol{\gamma} \in \Omega^2$, consider $\mathbf{j} = [1/2, 0]^T \in \Xi^{(1)} \setminus \Xi^{(0)}$ that belongs to the horizontal stencil $\mathcal{B}^{(0)}_{\mathbf{j}}$. If $\mathbf{f}^{(0)} = F(\Xi^{(0)})$ for some $F \in W_{\boldsymbol{\gamma}}$, $\boldsymbol{\gamma} \in \Omega^2$, it satisfies the system of equations given by (23) and (29), i.e.,

$$\begin{cases} \mathcal{N}_{\mathbf{j}-3\mathbf{e}_1/2-\mathbf{e}_2,\mathbf{e}_1+2\mathbf{e}_2,\mathbf{e}_1}\left(\boldsymbol{\gamma},\, \mathbf{f}^{(0)}|_{\mathcal{B}^{(0)}_{\mathbf{j}}}\right) \;=\; 0, \\ \mathcal{N}_{\mathbf{j}-\mathbf{e}_1/2-\mathbf{e}_2,\mathbf{e}_1,\mathbf{e}_2}\left(\boldsymbol{\gamma},\, \mathbf{f}^{(0)}|_{\mathcal{B}^{(0)}_{\mathbf{j}}}\right) \;=\; 0, \\ \mathcal{N}_{\mathbf{j}-3\mathbf{e}_1/2,\mathbf{e}_1,\mathbf{e}_1}\left(\boldsymbol{\gamma},\, \mathbf{f}^{(0)}|_{\mathcal{B}^{(0)}_{\mathbf{j}}}\right) \;=\; 0, \\ \mathcal{N}^+_{\mathbf{j}-3\mathbf{e}_1/2-\mathbf{e}_2,\mathbf{e}_1,\mathbf{e}_2,\mathbf{e}_1,\mathbf{e}_1+\mathbf{e}_2}\left(\boldsymbol{\gamma},\, \mathbf{f}^{(0)}|_{\mathcal{B}^{(0)}_{\mathbf{j}}}\right) \;=\; 0, \\ \mathcal{N}^-_{\mathbf{j}-3\mathbf{e}_1/2-\mathbf{e}_2,\mathbf{e}_1,\mathbf{e}_1,\mathbf{e}_2,\mathbf{e}_1+\mathbf{e}_2}\left(\boldsymbol{\gamma},\, \mathbf{f}^{(0)}|_{\mathcal{B}^{(0)}_{\mathbf{j}}}\right) \;=\; 0. \end{cases} \tag{32}$$

Thus, we can build a basis for the data according to next decomposition:

$$\mathbb{C}^{10} \;=\; W_{\boldsymbol{\gamma}}\left(\mathcal{B}^{(0)}_{\mathbf{j}}\right) \,\oplus\, W_{\boldsymbol{\gamma}}\left(\mathcal{B}^{(0)}_{\mathbf{j}}\right)^{\perp},$$

where

$$W_{\boldsymbol{\gamma}}\left(\mathcal{B}^{(0)}_{\mathbf{j}}\right) \;:=\; \left\{\; F\left(\mathcal{B}^{(0)}_{\mathbf{j}}\right) \;:\; F \in W_{\boldsymbol{\gamma}} \;\right\} \;\subset\; \mathbb{C}^{10}.$$

Now, it is straightforward to observe that the dimension of $W_{\boldsymbol{\gamma}}\left(\mathcal{B}_{\mathbf{j}}^{(0)}\right)$ is 5. As for equation (21) in Proposition 4.1, it is easy to see that the action of each of the 5 annihilators in (32) against $\mathbf{f}^{(0)}|_{\mathcal{B}_{\mathbf{j}}^{(0)}}$ is just the multiplication by a vector of coefficients belonging to $W_{\boldsymbol{\gamma}}\left(\mathcal{B}_{\mathbf{j}}^{(0)}\right)^{\perp}$. Then, since the chosen annihilators are linearly independent, a solution $(\boldsymbol{\gamma}_{hori}, \mathbf{p}) \in \Omega^2 \times \mathbb{C}^{10}$ to (32) implies the existence of a unique function $F \in W_{\boldsymbol{\gamma}_{hori}}$ such that $\mathbf{p} = \mathbf{f}^{(0)}|_{\mathcal{B}_{\mathbf{j}}^{(0)}}$, for $\mathbf{f}^{(0)} = F(\Xi^{(0)})$. For the sake of conciseness, the proof of their linear independence is omitted.

Remark 5.1. System (32) also solves the problem exposed in Remark 4.2. Indeed, if the first two equations of (32) can not be solved for $\boldsymbol{\gamma}$, one can actually choose any subset of equations in (32) in order to detect $\boldsymbol{\gamma}$. If this is not possible for any subset of equations, this means that (32) is satisfied by $(\boldsymbol{\gamma}, \mathbf{p})$ for all $\boldsymbol{\gamma} \in \Omega^2$, which implies $\mathbf{p}$ is obtained from the samples of a function F that belongs to all the spaces $W_{\boldsymbol{\gamma}}$, $\boldsymbol{\gamma} \in \Omega^2$. Thus, it does not matter which subdivision rule is used among (12) and (13) and which frequency $\boldsymbol{\gamma}$ is chosen: F will always be reproduced.

The same conclusions are achieved for the vertical case by $\mathbf{j} = [0, 1/2]^T \in \Xi^{(1)} \setminus \Xi^{(0)}$ and the system

$$\begin{cases} \mathcal{N}_{\mathbf{j}-\mathbf{e}_1-\mathbf{e}_2/2,\mathbf{e}_2,\mathbf{e}_1}\left(\boldsymbol{\gamma}_{vert}, \mathbf{p}\right) = 0, \\ \mathcal{N}_{\mathbf{j}-\mathbf{e}_1-3\mathbf{e}_2/2,2\mathbf{e}_1+\mathbf{e}_2,\mathbf{e}_2}\left(\boldsymbol{\gamma}_{vert}, \mathbf{p}\right) = 0, \\ \mathcal{N}_{\mathbf{j}-3\mathbf{e}_2/2,\mathbf{e}_2,\mathbf{e}_2}\left(\boldsymbol{\gamma}_{vert}, \mathbf{p}\right) = 0, \\ \mathcal{N}^{+}_{\mathbf{j}-\mathbf{e}_1-3\mathbf{e}_2/2,\mathbf{e}_2,\mathbf{e}_1,\mathbf{e}_2,\mathbf{e}_1+\mathbf{e}_2}\left(\boldsymbol{\gamma}_{vert}, \mathbf{p}\right) = 0, \\ \mathcal{N}^{-}_{\mathbf{j}-\mathbf{e}_1-3\mathbf{e}_2/2,\mathbf{e}_2,\mathbf{e}_2,\mathbf{e}_1,\mathbf{e}_1+\mathbf{e}_2}\left(\boldsymbol{\gamma}_{vert}, \mathbf{p}\right) = 0, \end{cases} \tag{33}$$

and for the diagonal case by $\mathbf{j} = [1/2, 1/2]^T \in \Xi^{(1)} \setminus \Xi^{(0)}$ and the system

$$\begin{cases} \mathcal{N}_{\mathbf{j}-3\mathbf{e}_1/2-\mathbf{e}_2/2,\mathbf{e}_1+\mathbf{e}_2,\mathbf{e}_1}\left(\boldsymbol{\gamma}_{diag}, \mathbf{p}\right) = 0, \\ \mathcal{N}_{\mathbf{j}-\mathbf{e}_1/2-3\mathbf{e}_2/2,\mathbf{e}_1+\mathbf{e}_2,\mathbf{e}_2}\left(\boldsymbol{\gamma}_{diag}, \mathbf{p}\right) = 0, \\ \mathcal{N}^{+}_{\mathbf{j}-3\mathbf{e}_1/2-3\mathbf{e}_2/2,\mathbf{e}_1+\mathbf{e}_2,\mathbf{e}_2,\mathbf{e}_1,\mathbf{e}_1+\mathbf{e}_2}\left(\boldsymbol{\gamma}_{diag}, \mathbf{p}\right) = 0, \\ \mathcal{N}^{+}_{\mathbf{j}-3\mathbf{e}_1/2-3\mathbf{e}_2/2,\mathbf{e}_1,\mathbf{e}_2,\mathbf{e}_1+\mathbf{e}_2,\mathbf{e}_1+\mathbf{e}_2}\left(\boldsymbol{\gamma}_{diag}, \mathbf{p}\right) = 0, \\ \mathcal{N}^{-}_{\mathbf{j}-3\mathbf{e}_1/2-3\mathbf{e}_2/2,\mathbf{e}_1,\mathbf{e}_1+\mathbf{e}_2,\mathbf{e}_2,\mathbf{e}_1+\mathbf{e}_2}\left(\boldsymbol{\gamma}_{diag}, \mathbf{p}\right) = 0. \end{cases} \tag{34}$$

Given $\mathbf{p} \in \mathbb{C}^{10}$ then one can proceed as follows. First, using the first two equations of each system (32), (33) and (34), one can compute, when possible, $\boldsymbol{\gamma}_{hori}$, $\boldsymbol{\gamma}_{vert}$ and $\boldsymbol{\gamma}_{diag}$ as done in (23), (24) and (25). Then, for each computed pair $(\boldsymbol{\gamma}_{hori}, \mathbf{p})$, $(\boldsymbol{\gamma}_{vert}, \mathbf{p})$ and $(\boldsymbol{\gamma}_{diag}, \mathbf{p})$, one can check if one of the systems (32), (33) and (34) is fully satisfied. If only one of them is satisfied, then we interpret the data as from an horizontal, vertical or diagonal stencil, respectively, and thus we use the corresponding subdivision rule. If more than one system is satisfied, it can be proved that all the corresponding subdivision rules give the same result for the newly inserted vertex. If none of them is satisfied it means that there is no function F in any of the spaces $W_{\boldsymbol{\gamma}}$, $\boldsymbol{\gamma} \in \Omega^2$, interpolating $\mathbf{p}$ over a stencil.

The previous strategy can be easily generalized for each subdivision level $k \in \mathbb{N}$, similarly to what has been done in Remark 4.3, and easily implemented. This yields a non-linear level-independent subdivision procedure able to reproduce locally functions from the spaces $\{W_{\boldsymbol{\gamma}}\}_{\boldsymbol{\gamma}\in\Omega^2}$, that can be turned into a scheme with some adjustments. The result of a first naive attempt to do so is shown in Figure 4, where the initial data on the left are sampled from a piecewise surface consisting of a sphere, a cylinder and a hyperboloid,

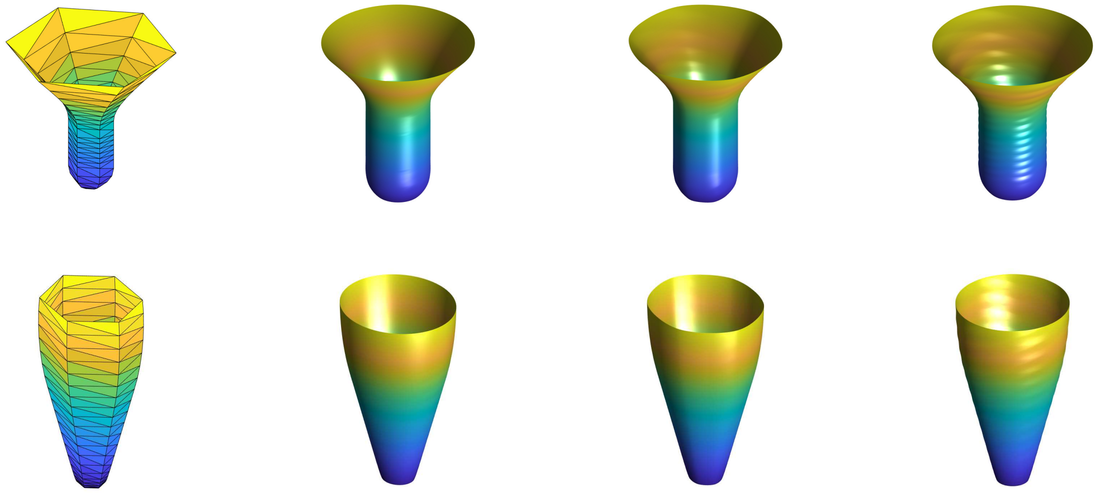

Figure 4: First row: a piecewise surface consisting of a sphere, a cylinder and a hyperboloid. Second row: a piecewise surface consisting of an ellipsoid, an elliptic cone and an elliptic hyperboloid. First column: the initial mesh. The other columns are subdivision reconstructions from this mesh after 5 subdivision steps. Second column: result of the procedure described in Example 5.1. Third column: result of the classical butterfly scheme. Last column: result of a level-dependent scheme reproducing the sphere/ellipsoid.

in the first row, and an ellipsoid, an elliptic cone and an elliptic hyperboloid, in the second row. Here, when none of the systems (32), (33) and (34) is satisfied, the classical butterfly scheme rule (7) is used.

To summarize what we learnt from Example 5.1: disposing of the right set of annihilators for a family of exponential polynomial spaces can give us the opportunity to detect the correct rule to use when different rules are applied to stencils with the same topological configuration. In particular, let, for every $t \in \mathcal{T}$, $\{\mathcal{N}_h^t\}_{h\in\mathcal{I}_t}$ ($\mathcal{I}_t$ being a set of indices) be a family of linear annihilators for the spaces $\{W_{\Gamma,M}\}_{(\Gamma,M)\in\widehat{\Omega}}$, that involves data over a single stencil of type t. Assume also that, for every $(\Gamma, M) \in \widehat{\Omega}$, $\dim(W_{\Gamma,M}) = N \in \mathbb{N}$. If, for every $t \in \mathcal{T}$, there are $H - N$ linearly independent annihilators in $\{\mathcal{N}_h^t\}_{h\in\mathcal{I}_t}$, those can be exploited to check the existence and uniqueness of a function F in a specific $W_{\Gamma,M}$ that interpolates a given vector of data $\mathbf{p} \in \mathbb{C}^H$ attached to the common configuration in $\mathcal{T}$. This, together with what has been discussed in Section 4, opens the possibility to construct a fully automatic subdivision scheme that is able to locally detect the type of stencil and the corresponding rules to reproduce all the exponential polynomials belonging to the family of spaces $\{W_{\Gamma,M}\}_{(\Gamma,M)\in\widehat{\Omega}}$. As shown in Example 5.1, one can proceed as follows: for every set of data fitting in a stencil,

if we are able to extract from the annihilators a unique value for (Γ, M) and t, with a well-defined associated non-linear rule that reproduces $W_{(\Gamma,M)}$,

then we use that particular subdivision rule on the data;

else we use the subdivision rule of a fixed scheme, e.g. the classical butterfly scheme.

However, one has to be aware that the convergence of such a subdivision procedure is not guaranteed and must be studied separately, along with its behaviour in the transition region between the samples of exponential polynomials belonging to different spaces.

Acknowledgments

The first author was supported by the research project MTM2017-83942-P (Ministry of Economy and Competitivity, MINECO, Spain), the FPU14/02216 grant and the EST16/00133 short stays scholarship

(Ministry of Education and Culture and Sports, MECD, Spain).

The second author acknowledges support from GNCS-INdAM within the research project entitled *Interpolation and Smoothing: Theoretical, Computational and Applied Aspects*.

This work born within the frameworks of the *Research ITalian network of Approximation* (RITA) and of the group *Teoria dell'Approssimazione e Applicazioni* (TAA) at the *Unione Matematica Italiana* (UMI).

References

Albrecht, G., Romani, L., 2012. Convexity preserving interpolatory subdivision with conic precision. Appl. Math. Comput. 219, 4049–4066.

Badoual, A., Novara, P., Romani, L., Schmitter, D., Unser, M., 2017a. A non-stationary subdivision scheme for the construction of deformable models with sphere-like topology. Graph. Models 94, 38–51.

Badoual, A., Schmitter, D., Uhlmann, V., Unser, M., 2017b. Multiresolution subdivision snakes. IEEE Trans. Image Process. 26, 1188–1201.

Beccari, C., Casciola, G., Romani, L., 2007. A non-stationary uniform tension controlled interpolating 4-point scheme reproducing conics. Comput. Aided Geom. Design 24, 1–9.

Beccari, C., Casciola, G., Romani, L., 2009. Shape controlled interpolatory ternary subdivision. Appl. Math. Comput. 215, 916–927.

Beccari, C.V., Casciola, G., Romani, L., 2010. A unified framework for interpolating and approximating univariate subdivision. Appl. Math. Comput. 216, 1169–1180.

Campagna, R., Conti, C., Cuomo, S., 2020. Computational error bounds for Laplace transform inversion based on smoothing splines. Appl. Math. Comput. 383, 125376, 11.

Chalmovianský, P., Jüttler, B., 2007. A non-linear circle-preserving subdivision scheme. Adv. Comput. Math. 27, 375–400.

Charina, M., Conti, C., 2013. Polynomial reproduction of multivariate scalar subdivision schemes. J. Comput. Appl. Math. 240, 51–61.

Charina, M., Conti, C., Sauer, T., 2005. Regularity of multivariate vector subdivision schemes. Numer. Algorithms 39, 97–113.

Conti, C., Cotronei, M., Sauer, T., 2016a. Factorization of Hermite subdivision operators preserving exponentials and polynomials. Advances in Computational Mathematics 42, 1055–1079.

Conti, C., Deng, C., Hormann, K., 2018. Symmetric four-directional bivariate pseudo-spline symbols. Comput. Aided Geom. Design 60, 10–17.

Conti, C., Donatelli, M., Romani, L., Novara, P., 2019. Convergence and normal continuity analysis of nonstationary subdivision schemes near extraordinary vertices and faces. Constr. Approx. 50, 457–496.

Conti, C., Gemignani, L., Romani, L., 2011. From approximating to interpolatory non-stationary subdivision schemes with the same generation properties. Adv. Comput. Math. 35, 217–241.

Conti, C., López-Ureña, S., Romani, L., 2020. Annihilation operators for exponential spaces in subdivision. arXiv 2012.09485.

Conti, C., Romani, L., 2010. Affine combination of B-spline subdivision masks and its non-stationary counterparts. BIT 50, 269–299.

Conti, C., Romani, L., Unser, M., 2015. Ellipse-preserving Hermite interpolation and subdivision. J. Math. Anal. Appl. 426, 211–227.

Conti, C., Romani, L., Yoon, J., 2016b. Approximation order and approximate sum rules in subdivision. J. Approx. Theory 207, 380–401.

Deng, C., Wang, G., 2010. Incenter subdivision scheme for curve interpolation. Comput. Aided Geom. Design 27, 48–59.

Donat, R., López-Ureña, S., 2019. Nonlinear stationary subdivision schemes reproducing hyperbolic and trigonometric functions. Adv. Comput. Math. 45, 3137–3172.

Dyn, N., Levin, D., Gregory, J.A., 1990. A butterfly subdivision scheme for surface interpolation with tension control. ACM Trans. Graph. 9, 160–169.

Dyn, N., Levin, D., Luzzatto, A., 2003. Exponentials reproducing subdivision schemes. Found. Comput. Math. 3, 187–206.

Jeong, B., Kim, H.O., Lee, Y.J., Yoon, J., 2013. Exponential polynomial reproducing property of non-stationary symmetric subdivision schemes and normalized exponential B-splines. Adv. Comput. Math. 38, 647–666.

Lee, Y.J., Yoon, J., 2010. Non-stationary subdivision schemes for surface interpolation based on exponential polynomials. Appl. Numer. Math. 60, 130–141.

Levin, A., 2005. The importance of polynomial reproduction in piecewise-uniform subdivision, in: Mathematics of Surfaces XI. Springer, pp. 272–307.

Li, X., Kong, L., Cheng, J., Wu, L., 2015. The study of NMR relaxation time spectra multi-exponential inversion based on Lloyd–Max optimal quantization. Journal of Geophysics and Engineering 12, 144–153.

Michálková, K., Bastl, B., 2015. A tetrahedron-based subdivision scheme for spatial G^1 curves. J. Comput. Appl. Math. 281, 196–206.

Novara, P., Romani, L., 2015. Building blocks for designing arbitrarily smooth subdivision schemes with conic precision. J. Comput. Appl. Math. 279, 67–79.

Novara, P., Romani, L., Yoon, J., 2016. Improving smoothness and accuracy of modified butterfly subdivision scheme. Appl. Math. Comput. 272, 64–79.

Romani, L., 2010. A circle-preserving C^2 Hermite interpolatory subdivision scheme with tension control. Comput. Aided Geom. Design 27, 36–47.

Romani, L., Hernández Mederos, V., Estrada Sarlabous, J., 2016. Exact evaluation of a class of nonstationary approximating subdivision algorithms and related applications. IMA J. Numer. Anal. 36, 380–399.

Sabin, M.A., Dodgson, N.A., 2005. A circle-preserving variant of the four-point subdivision scheme, in: Mathematical methods for curves and surfaces: Tromsø 2004. Nashboro Press, Brentwood, TN. Mod. Methods Math., pp. 275–286.

Uhlmann, V., Delgado-Gonzalo, R., Conti, C., Romani, L., Unser, M., 2014. Exponential Hermite splines for the analysis of biomedical images, in: 2014 IEEE International Conference on Acoustics, Speech and Signal Processing (ICASSP), pp. 1631–1634.